

Refraction of radio waves in pulsar magnetospheres

Y.E. Lyubarskii and S.A. Petrova

Institute of Radio Astronomy, Chervonopraporna St.4, Kharkov, 310002, Ukraine

Received 4 July 1997/ Accepted 5 January 1998

Abstract. Influence of refraction on the pulse width versus frequency curve is considered. Radio waves are assumed to be emitted from a range of altitudes at frequencies of the order of local Lorentz-shifted proper plasma frequencies. It is shown that refraction may account for the so called "absorption feature" on the observed pulse width versus frequency curve and also for the observed frequency dependence of separation between components of double profiles.

Key words: plasmas – waves – pulsars: general

1. Introduction

Pulsar magnetospheres are believed to be filled with an ultrarelativistic electron-positron plasma streaming along the open field lines of a superstrong magnetic field. Radiation from this plasma is collimated into a narrow beam directed along the magnetic axis. The beam width may be affected by refraction. A general theory of radio wave refraction in an ultrarelativistic plasma embedded in a superstrong dipole magnetic field was developed by Barnard & Arons (1986). These authors applied general equations to the case when the waves in the whole observed range of frequencies are emitted at one altitude in the open field line tube, that is at one density of a medium. Since refractive index depends on ω/ω_p , it turns out that the lower the frequency, the stronger refraction. Hence, at low frequencies the beam widens with the wavelength while at high frequencies the beam width remains nearly constant. Many pulsars indeed exhibit such a behaviour.

The aim of this research is to consider refraction of rays originated within a range of altitudes at frequencies of the order of the local Lorentz-shifted proper plasma frequencies

$$\omega_0 = \omega_p \sqrt{\gamma}, \quad (1.1)$$

where γ is the plasma Lorentz-factor, ω_p given by the customary expression

$$\omega_p = \sqrt{\frac{4\pi N e^2}{m}} \quad (1.2)$$

with N being the plasma number density, m the electron mass. The frequency (1.1) is set off because waves excited in pul-

sar plasma seek this frequency in the course of induced scatterings (Lyubarskii 1996). At wave energy densities consistent with the observed pulsar luminosities this process should be rather efficient. Let for example two-stream instability be a source of pulsar radio emission (Usov 1987; Ursov & Usov 1988; Lyubarskii 1992a,b, 1993). In this case subluminal longitudinal waves are excited and induced scattering transforms these waves into superluminal ones which ultimately escape from the magnetosphere in a form of transverse electromagnetic waves (Lyubarskii 1996; Bliokh & Lyubarskii 1996).

So the case $\omega \sim \omega_0$ seem to be of special interest. The plasma density inside the open field line tube decreases with the distance from the neutron star, therefore radiation at a given frequency is emitted at corresponding radius, $\nu \propto r^{-3/2}$ (radius-to-frequency mapping). In this case neglect of refraction implies the pulse width $w \propto \nu^{-1/3}$. The observed pulse width does increase with the wavelength, however, the frequency dependence of the pulse width does not follow the above universal law. The pulse widths of many pulsars are nearly constant at high frequencies and increase at low ones (Rankin 1983). At frequencies lower than 1 GHz the frequency dependence of the pulse width for some pulsars exhibits a trough which is called "the absorption feature" (Bartel 1981; Rankin 1983). However, up to date no appropriate mechanisms are suggested to account for such a feature. The only absorption mechanism in pulsar magnetospheres is the cyclotron absorption (Blandford & Scharlemann 1976; Mikhailovskii et. al. 1982). However, the cyclotron resonance occurs at radii of the order of the light cylinder radius where the width of the open field line tube, and correspondingly the characteristic scale of varying the absorption depth, significantly exceeds the beam width. Therefore the cyclotron absorption is hardly to be responsible for absorption of only a part of the beam.

We show that in case radius-to-frequency mapping, $\omega \sim \omega_0$, asserts refraction may account for the features of the observed pulse width versus frequency curves. In Sect. 2 we examine the system of Hamilton's equations for the ray propagation in the ultrarelativistic plasma streaming along the open field lines of an infinitely strong dipole magnetic field. The main features of ray behaviour at such conditions are outlined. Sect. 3 is devoted to investigating the observational consequences of refraction in pulsar magnetospheres. The pulse width versus frequency de-

pendence calculated allowing for refraction are compared with the observed curves. The results are summarized in Sect. 4.

2. Propagation of rays through the open field line tube

2.1. Hamilton's equations

Let us consider the propagation of an ordinary superluminal wave through an ultrarelativistic plasma streaming along the field lines of an infinitely strong magnetic field. For the sake of simplicity the plasma is assumed to be cold; all plasma particles move with an ultrarelativistic velocity characterized by the Lorentz-factor γ . The dispersion relation for the ordinary waves in such a plasma is as follows (see, e.g., review by Lyubarskii 1995):

$$(1 - n_{\parallel}^2) \left(1 - \frac{\omega_p^2}{\omega^2 \gamma^3 (1 - n_{\parallel} \beta)^2} \right) - n_{\perp}^2 = 0, \quad (2.1)$$

where $n_{\parallel} = ck_{\parallel}/\omega$, $n_{\perp} = ck_{\perp}/\omega$, with k_{\parallel} , k_{\perp} being the wave vector components parallel and perpendicular to the magnetic field, respectively, β is the plasma particle velocity in units of c .

All the scale lengths supposed in the typical pulsar models are much larger than the observed radio wavelengths, so the geometrical optics approximation is valid. Evolution of the wave packet coordinate \mathbf{x} and momentum \mathbf{k} can be described by the system of Hamilton's equations:

$$\frac{d\mathbf{x}}{dt} = -\frac{\partial D/\partial \mathbf{k}}{\partial D/\partial \omega},$$

$$\frac{d\mathbf{k}}{dt} = \frac{\partial D/\partial \mathbf{x}}{\partial D/\partial \omega},$$

where t is the time elapsed since the wave packet have been created, $D(\mathbf{x}, \mathbf{k}, \omega)$ the dispersion relation of a medium. Given the dispersion relation (2.1) is the case Barnard & Arons (1986) reduced these equations to the form:

$$\frac{1}{c} \frac{d\mathbf{x}}{dt} = p\mathbf{n} - q\mathbf{b}, \quad (2.2)$$

$$\frac{1}{\omega} \frac{d\mathbf{k}}{dt} = q \frac{\partial \mathbf{b}}{\partial \mathbf{x}} \cdot \mathbf{n} - l \frac{\partial \ln N}{\partial \mathbf{x}}. \quad (2.3)$$

Here \mathbf{n} , \mathbf{b} are unit vectors aligned with \mathbf{k} and magnetic field, respectively,

$$\begin{aligned} p &= (1 + \eta)^3/d, & q &= 4(1 - \eta)/(\Omega^2 d), \\ l &= 2(1 + \eta)(1 - n_{\parallel}^2)/(\Omega^2 d), & \eta &= 2\gamma^2(1 - n_{\parallel}), \\ d &= (1 + \eta)^3 - 4(1 - \eta)(1 - \eta/(2\gamma^2))/\Omega^2, \end{aligned}$$

with

$$\Omega = \omega/\omega_0 \quad (2.4)$$

being the frequency in units of the local plasma frequency (1.1). Note that the above definition of d as well as the numerators of p , q , l differ from those given by Barnard & Arons, the former being normalized by the $8\gamma^3$ factor. Then these quantities are

of the order of unity as we are considering the waves originated at frequencies close to the local plasma frequency.

We suppose magnetic field to be dipole with the axis aligned with the z -axis of the two-dimensional Cartesian coordinate system. Since the open field line tube is narrow the field components may be written as

$$B_y = \frac{3}{2} B_0 \frac{zy}{r^2} \left(\frac{r_{\star}}{r} \right)^3, \quad B_z = B_0 \left(1 - \frac{9y^2}{8r^2} \right) \left(\frac{r_{\star}}{r} \right)^3, \quad (2.5)$$

where r_{\star} is the radius of the neutron star, B_0 the field strength at the stellar surface.

Continuity of the plasma flow within the open field line tube requires the plasma number density to follow the magnetic field strength,

$$N = N_0 \left(\frac{r_{\star}}{r} \right)^3, \quad (2.6)$$

where N_0 is the number density at the bottom of the field line tube. Of course, the plasma number density varies across the tube as well. Transverse density gradient is expected to be essentially larger than radial one since the transverse scale of the open field line tube is small compared with the radial one.

In the dipole case the angle the field line makes with the magnetic axis is $\approx 3\vartheta/2$, with ϑ being the polar angle of the point, $\vartheta \approx y/z$. Note that ϑ is small for the open field lines well within the magnetosphere. The ray is supposed to be emitted along the field line, the initial value of n_{\perp} being zero. One can expect that n_{\perp} varies within the order of ϑ in magnitude while the ray is affected by the plasma. Thus ϑ and n_{\perp} may be considered as small parameters.

To the first order in ϑ and n_{\perp} the system (2.2)–(2.3) may be rewritten as

$$\frac{1}{c} \frac{dr}{dt} = pn_{\parallel} - q, \quad (2.7)$$

$$\frac{r}{c} \frac{d\vartheta}{dt} = \frac{\vartheta}{2} (pn_{\parallel} - q) - pn_{\perp}, \quad (2.8)$$

$$\frac{1}{c} \frac{dn_y}{dt} = -\frac{3qn_{\perp}}{2r} + \frac{3l\vartheta}{r} - \frac{l}{r} \frac{\partial \ln N}{\partial \vartheta}, \quad (2.9)$$

$$\frac{1}{c} \frac{dn_z}{dt} = \frac{3l}{r} + \frac{l\vartheta}{r} \frac{\partial \ln N}{\partial \vartheta}. \quad (2.10)$$

Some further simplification of the system is possible. One of the equations of the system, namely the last one, may be replaced by the dispersion relation (2.1). Time dependence may be eliminated through division of the system equations by the first one. The wave vector of a ray makes an angle $(3\vartheta/2 - n_{\perp})$ with the magnetic axis at each point of the trajectory; then the deviation of the wave vector from its initial direction is given by

$$\zeta = 3(\vartheta - \vartheta_0)/2 - n_{\perp}. \quad (2.11)$$

Here $\vartheta_0 = y_0/z_0$ is the polar angle of the emission point and $n_{\perp 0}$ is assumed to be zero.

Taking into account the above considerations yields:

$$r \frac{d\zeta}{dr} = \frac{3q[3(\vartheta_0 - \vartheta)/2 + \zeta]}{2(pn_{\parallel} - q)} + \frac{3l\vartheta}{(pn_{\parallel} - q)} - \frac{l}{(pn_{\parallel} - q)} \frac{\partial \ln N}{\partial \vartheta},$$

$$r \frac{d\vartheta}{dr} = \frac{\vartheta}{2} - \frac{p[3(\vartheta - \vartheta_0)/2 - \zeta]}{(pn_{\parallel} - q)},$$

$$\eta \left(1 - \frac{4}{\Omega^2(1 + \eta)^2} \right) \left(1 - \frac{\eta}{4\gamma^2} \right) = n^2,$$

where $n = n_{\perp}\gamma$. Recalling the definitions listed after Eq. (2.3) and using Eq. (2.6) we find finally:

$$r \frac{d\zeta}{dr} = \frac{6(r/r_0)^{-3}N(\vartheta)}{A\Omega_0^2N(\vartheta_0)} \left\{ (1 - \eta) \left[\frac{3(\vartheta_0 - \vartheta)}{2} + \zeta \right] + \frac{\vartheta\eta(1 + \eta)}{\gamma^2} - \frac{\eta(1 + \eta)}{3\gamma^2} \frac{\partial \ln N}{\partial \vartheta} \right\}, \quad (2.12)$$

$$r \frac{d\vartheta}{dr} = \frac{\vartheta}{2} - \frac{(1 + \eta)^3}{A} \left[\frac{3(\vartheta - \vartheta_0)}{2} - \zeta \right], \quad (2.13)$$

$$\eta \left(1 - \frac{4(r/r_0)^{-3}N(\vartheta)}{\Omega_0^2N(\vartheta_0)(1 + \eta)^2} \right) \left(1 - \frac{\eta}{4\gamma^2} \right) = n^2, \quad (2.14)$$

where

$$A = (1 + \eta)^3 \left(1 - \frac{\eta}{2\gamma^2} \right) - \frac{4(r/r_0)^{-3}(1 - \eta)N(\vartheta)}{\Omega_0^2N(\vartheta_0)}$$

and all the quantities referring to the emission point are subscripted with 0. The system (2.12) – (2.14) describes the ray trajectory and wave vector evolution during the propagation along the open field line tube.

2.2. Wave vector deviation

At first we examine ray equations (2.12) – (2.14) to outline some general features of the ordinary superluminal wave behaviour while it is propagating through the ultrarelativistic plasma embedded in the superstrong dipole magnetic field. The ray is assumed to be emitted along the magnetic field line at the frequency of the order of the local plasma frequency (1.1) at the point of generation. Since the plasma number density given by Eq. (2.6) decreases along the ray trajectory the local plasma frequency becomes lower than the ray frequency and the plasma influence on the ray ultimately ceases. According to Eq. (2.14), at large distances the refractive index of the ordinary superluminal wave approaches unity and the rate of variation of the wave vector approaches zero, the wave becoming a vacuum electromagnetic wave unaffected by the plasma. So refraction is efficient only at distances comparable to the emission radius r_0 . We are interested in the wave vector deviation from its initial direction ζ since ultimately the ray becomes aligned with the wave vector; therefore ζ is the quantity that characterizes the influence of refraction on the observed pulse width of the pulsar.

The refractive index varies along the ray trajectory due to varying both the plasma density and angle the wave vector makes with the magnetic field because of field line curvature. This is indicated explicitly by the right-hand side of Eq. (2.3). The first term in the parentheses of Eq. (2.12) represents the contribution of field line curvature to refraction while the other two ones refer to density variation along the trajectory. Note

that the second term, which is the y -component of radial density gradient, is γ^2 less than the first one and ϑ^{-2} less than the third one. So the contribution of radial density gradient to refraction is negligible. The contribution of field line curvature to refraction appears to be insignificant as well. The matter is that it is of the order of n_{\perp} which increases to $\sim \vartheta_0$ only at distances where refraction ceases. At small polar angles, $\vartheta \lesssim 1/\gamma$, transverse density gradient contributes essentially to refraction. The behaviour of a ray should depend qualitatively on transverse plasma density gradient.

The plasma inside the open field line tube is believed to originate in a polar gap due to conversion of gamma-photons. Curvature of magnetic field lines is of crucial importance for this process. Since the field lines located close to the magnetic axis are nearly straight ones there would be no secondary plasma in that region. For a lack of plasma close to the magnetic axis as well as out of the open field line tube both inward and outward transverse density gradients seem to exist inside the tube. Furthermore, it should be noticed that plasma generation is supposed to be unsteady. So one might expect that at any instant the plasma is concentrated in some narrow tubes within the open field line tube. Then the scale length of transverse density gradient is less than the open field line tube width. Below we consider refraction of rays inside the open magnetic line tube in two idealized cases of monotone inward and outward plasma density decrease.

2.2.1. Outward density decrease

Now we investigate refraction of rays emitted at distance of the order of the open field line tube width from the magnetic axis and propagating through the plasma which number density falls towards the tube edge. Let the plasma density be given by

$$N = \frac{N_0}{1 + \varepsilon(\vartheta/\vartheta_c)^2} \left(\frac{r_{\star}}{r} \right)^3, \quad (2.15)$$

where $\vartheta_c = s/r$, with s being of the order of the tube width. Then

$$\frac{\partial \ln N}{\partial \vartheta} = -\frac{\varepsilon}{\vartheta_c} \frac{2\vartheta/\vartheta_c}{1 + \varepsilon(\vartheta/\vartheta_c)^2} \quad (2.16)$$

The third term in the parentheses of Eq. (2.12) makes the wave vector deviate away from the magnetic axis. If transverse density gradient is small ($\varepsilon \ll 1$) the right-hand side of Eq. (2.16) is negligible and transverse gradient does not contribute to refraction. Given that transverse density variation is rapid ($\varepsilon \gg 1$) $\frac{\partial \ln N}{\partial \vartheta}$ is independent on ε so that the wave vector deviation remains finite at $\varepsilon \rightarrow \infty$. The smaller initial polar angle ϑ_0 of the ray the stronger the wave vector deviates and the smaller values of n_{\perp} are approached. The rate of wave vector deviation is slowing down along the trajectory due to both radial density fall and transverse gradient decrease.

The wave vector deviation with radius found through the numerical solution of the system (2.12) – (2.14) is shown in Fig. 1. Here we take $\gamma = 30$, $\varepsilon = 1$, $\Omega_0 = 0.3$. The curves for $\vartheta_0 = 0.01, 0.03$ and 0.05 are plotted. In Fig. 1a one can see that along the trajectory the wave vector deviation is increasing

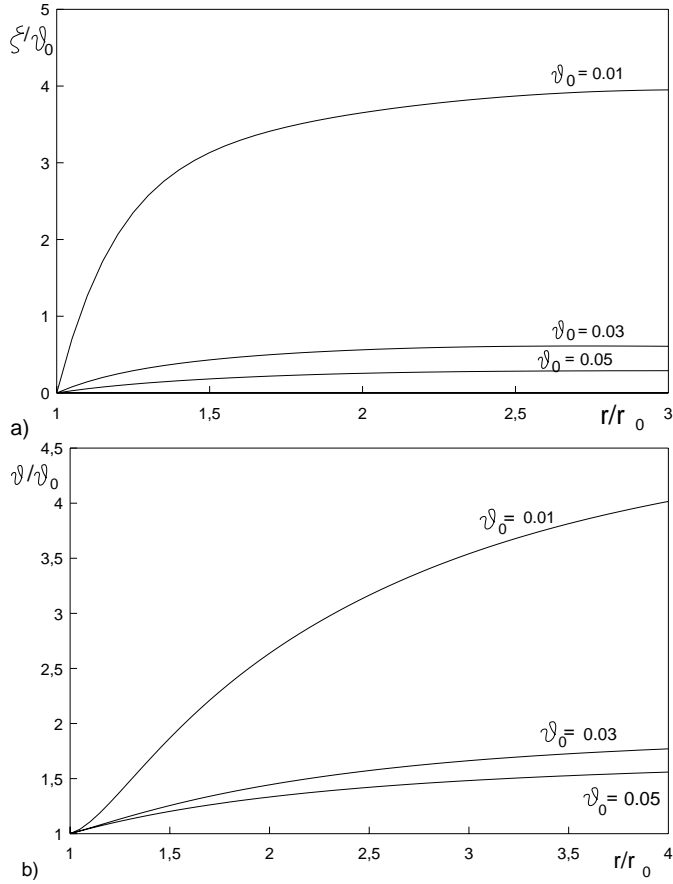


Fig. 1a and b. Ray behaviour in plasma with outward density decrease: **a** wave vector deviation vs. radius, **b** ray trajectories; $\gamma = 30$, $\varepsilon = 1$, $\Omega_0 = 0.3$

monotonically until it becomes constant. Refraction turns out to be significant only for the rays emitted at $\vartheta_0 \lesssim 1/\gamma$. The ray trajectories are given in Fig. 1b. They appear to deviate monotonically away from the magnetic axis. As it follows from Eq. (2.13), the polar angle of the trajectory increases with radius more rapidly for the rays emitted at smaller polar angles since in that case n_\perp is smaller.

Note that we are only interested in the final wave vector deviation of the outgoing ray since it determines the observed pulse width. In Fig. 2 we give the final ray deviation versus emission angle curves for various sets of parameters. According to Fig. 2a, refraction turns out to be more efficient at lower dimensionless frequency Ω_0 . Firstly, the rate of wave vector deviation is $\propto \Omega_0^{-2}$ (see Eq. (2.12)). Secondly, the lower Ω_0 the longer the ray interacts with the plasma. In fact, refraction occurs until the first parentheses in the dispersion relation (2.14) become close to unity; then $(1 - n_\parallel) \approx n_\perp^2/2$ implying that the wave decouples from the plasma. It is clear from Eq. (2.14) that the lower Ω_0 the later decoupling occurs. Fig. 2b illustrates the influence of parameter ε on the final ray deviation. Obviously, the steeper transverse density gradient (the larger ε) the larger deviation the ray undergoes. Note that although the refractive index slightly differs from unity, $\Delta n \sim 1/\gamma^2$, refraction appears to be not

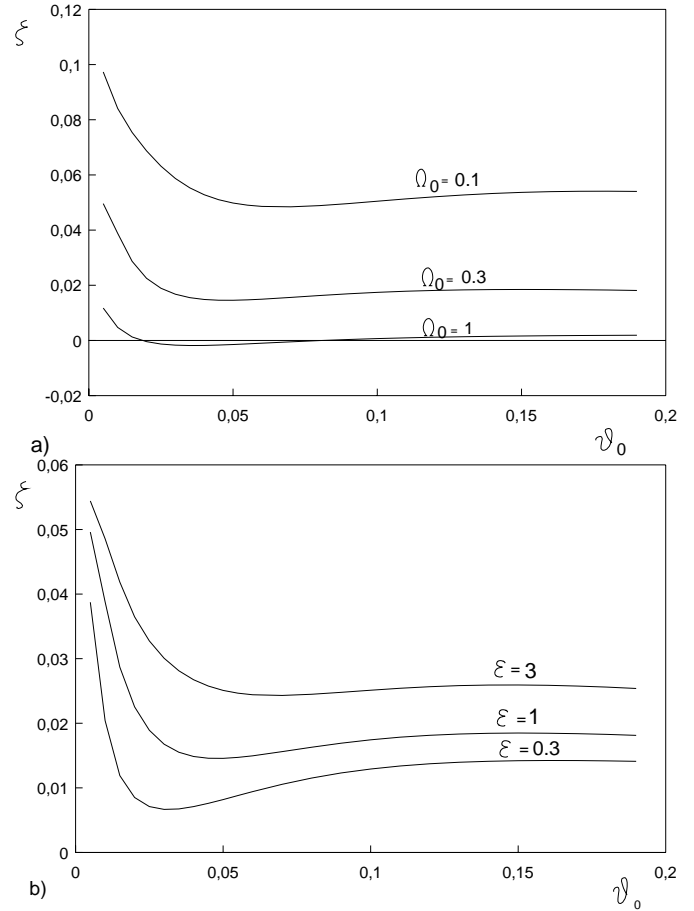


Fig. 2a and b. Final ray deviation vs. emission angle for various parameters: **a** $\varepsilon = 1$, **b** $\Omega_0 = 0.3$; $\gamma = 30$

very small since the ray propagates almost perpendicularly to the density gradient.

2.2.2. Density increasing outwards

Now let us consider the behaviour of rays propagating in the plasma which number density increases outwards from the magnetic axis:

$$N = N_0(1 + \varepsilon(\vartheta/\vartheta_c))(r_*/r)^3. \quad (2.17)$$

Outward transverse density gradient causes wave vector deviation towards the axis (see Eq. (2.12)). Thus n_\perp increases along the ray trajectory due to both magnetic line curvature and wave vector deviation. Apparently, the latter decreases with the emission angle ϑ_0 . For the rays with $\vartheta_0 > 1/\gamma$ n_\perp remains small enough providing trajectory bending away from the magnetic axis (see Eq. (2.13)). The trajectories of rays emitted at $\vartheta_0 < 1/\gamma$ curve towards the axis. If the wave vector deviation is sufficiently efficient the trajectory can intersect the magnetic axis and get to the region where transverse density gradient changes the sign. So the wave vector starts to deviate in the opposite direction. This deviation together with magnetic line curvature make n_\perp acquire negative values, the latter causing

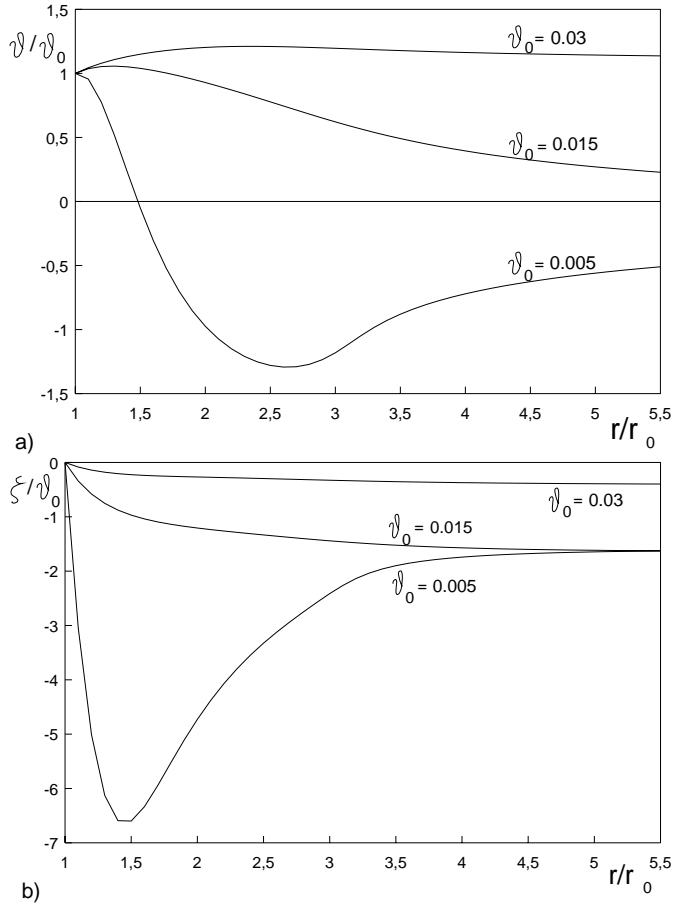


Fig. 3a and b. Ray behaviour in plasma with outward density increase: **a** ray trajectories, **b** wave vector deviation vs. radius; $\gamma = 30$, $\varepsilon = 10$, $\Omega_0 = 0.3$

trajectory bending towards the axis. Thus the trajectory can repeatedly intersect the magnetic axis.

Ray trajectories obtained through numerical solution of the system (2.12) – (2.14) with the plasma number density given by Eq. (2.17) are plotted in Fig. 3a. One can see that the trajectory of a ray emitted at $\vartheta_0 = 0.05$ ($\vartheta_0 > 1/\gamma$) bends away from the magnetic axis while in the case of $\vartheta_0 < 1/\gamma$ the trajectories start curving towards the axis. For the assumed set of parameters ($\gamma = 30$, $\Omega_0 = 0.3$, $\varepsilon = 10$) the trajectory of a ray emitted at $\vartheta_0 = 0.005$ intersects the magnetic axis before the ray decouples from the plasma. The wave vector deviation with radius is shown in Fig. 3b. For the rays emitted at $\vartheta_0 = 0.015$ and $\vartheta_0 = 0.05$ wave vector deviation towards the magnetic axis increases monotonically with radius due to transverse density gradient. As for the ray with $\vartheta_0 = 0.005$ its wave vector deviates towards the axis until the trajectory intersects the latter; then \mathbf{k} starts deviating in the opposite direction, that is again towards the axis.

The final ray deviation versus emission angle curves for various values of Ω_0 and ε are presented in Fig. 4. Given $\Omega_0 = 1$ the rays emitted at small polar angles ($\vartheta_0 \lesssim 1/\gamma$) suffer deviation towards the magnetic axis; the smaller the emission angle the stronger the deviation. For the rays originated at $\Omega_0 = 0.3$,

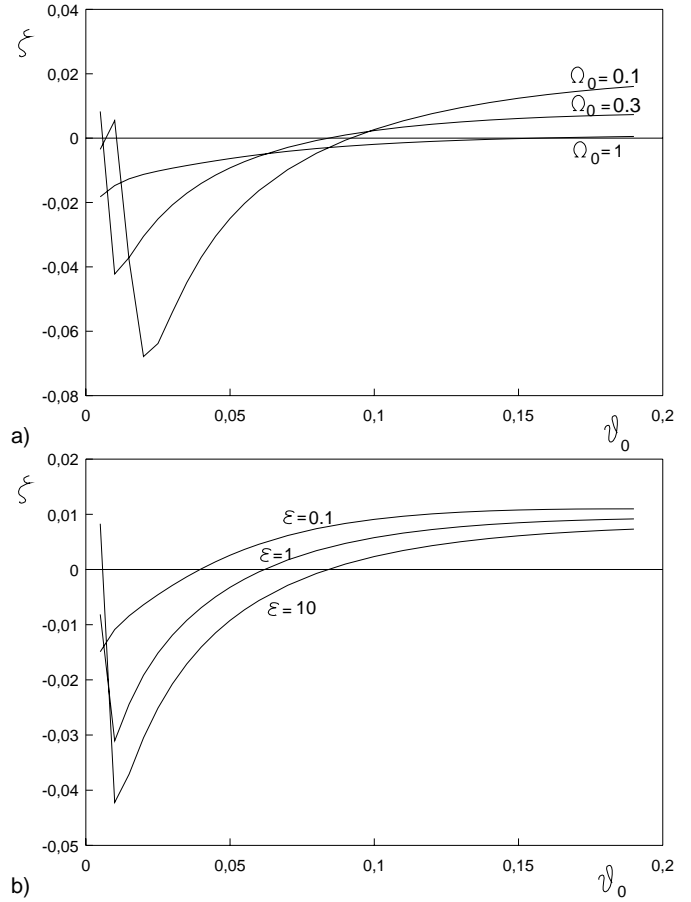


Fig. 4a and b. Final ray deviation vs. emission angle for various parameters: **a** $\varepsilon = 10$, **b** $\Omega_0 = 0.3$; $\gamma = 30$

$\vartheta_0 < 0.01$ the final deviation towards the axis decreases with decreasing ϑ_0 . This implies that the rays have time to intersect the axis and deviate in the opposite direction due to transverse density gradient beyond the axis. One more extremum on the curve for $\Omega_0 = 0.1$ indicates that the rays emitted at the smallest polar angles intersect the axis twice. Fig. 4b illustrates that refraction is less efficient for the smaller transverse density gradients (the smaller ε); this agrees with the discussed above.

3. Observational consequences of refraction in pulsar magnetospheres

In the previous section refraction of rays propagating through the plasma in the open field line tube is found to be significant. Now we turn to investigation of observational consequences of the effect in pulsar magnetospheres. Suppose that the ray is emitted near the local plasma frequency. So each frequency originates at different radius, with $\nu \propto r^{-3/2}$ (radius-to-frequency mapping), since the plasma density falls inside the open field line tube as r^{-3} . In the case of a magnetic dipole the polar angle ϑ of the field line increases with radius as $r^{1/2}$. Since we assume the rays to be emitted along the field lines, that is at the angle $\approx 3\vartheta/2$ to the magnetic axis, the pulse width without refraction would be: $w \propto r^{1/2} \propto \nu^{-1/3}$. Refraction of rays in the

open field line tube of a pulsar should affect the observed pulse width. Taking into account the strong dependence of refraction on initial polar angle of a ray one can expect that the frequency dependence of pulse width differs from the $\nu^{-1/3}$ law.

Now we proceed to a quantitative consideration. The plasma density at the stellar surface is conveniently normalized by the Goldreich-Julian charge density:

$$N_0 = \frac{\kappa B_0}{ceP}. \quad (3.1)$$

Here κ is the multiplicity factor, P the pulsar period, B_0 the magnetic field strength at the surface. Substituting Eq. (3.1) into Eq. (2.6) yields:

$$N = 6.25 \cdot 10^{13} P^{-1} \left(\frac{\kappa}{10^3} \right) \left(\frac{B_0}{10^{12} \text{G}} \right) \left(\frac{r_*}{r} \right)^3 \text{cm}^{-3}. \quad (3.2)$$

The ray is supposed to be emitted at the frequency $\omega = \Omega_0 \omega_{p0} \sqrt{\gamma}$, with the plasma frequency ω_{p0} given by Eq. (1.2). In the dipole case the polar angle of the last open field line is

$$\vartheta_t = \sqrt{\frac{r}{r_L}}, \quad (3.3)$$

where $r_L = 5 \cdot 10^9 P \text{cm}$ is the radius of a light cylinder. So the observed frequency ν is related to the initial polar angle of the boundary ray ϑ_0 by

$$\begin{aligned} \nu &= 2\Omega_0 P^{-2} \vartheta_0^{-3} \left(\frac{\kappa}{10^3} \right)^{1/2} \left(\frac{\gamma}{100} \right)^{1/2} \\ &\times \left(\frac{B_0}{10^{12} \text{G}} \right)^{1/2} \left(\frac{r_*}{10^6 \text{cm}} \right)^{3/2} \text{MHz}. \end{aligned} \quad (3.4)$$

The beam half-width is given by

$$w = 3\vartheta_0/2 + \zeta. \quad (3.5)$$

Note that it is not the observed FWHM even if the sight line scans the open field line tube across a diameter. The true FWHM may be found only if the radiation intensity distribution across the open field line tube is given, then the pulse shape could be calculated. We only calculate the angles which rays originated at different radii on the chosen magnetic field line eventually make with the axis. We believe that this gives, taking into account radius-to-frequency mapping, qualitative behaviour of the observed pulse width versus frequency curve. The field line which polar angle ϑ_0 is equal to the characteristic scale of density variation ϑ_c (see Eqs. (2.15), (2.17)), with $\vartheta_c = \vartheta_t/2$, is considered.

As we discussed above, the rays propagating in the plasma with an outward density decrease tend to deviate away from the magnetic axis. At low altitudes where high frequencies are believed to be emitted the angular width of the open magnetic flux tube, $3\vartheta_0/2$, is small and the contribution of refraction to the beam width is significant. At higher altitudes ϑ_0 increases, refraction becoming less significant; therefore at lower frequencies the beam width is mainly determined by the tube width and, correspondingly, increases with the wavelength. So at high frequencies the pulse width remains approximately constant while

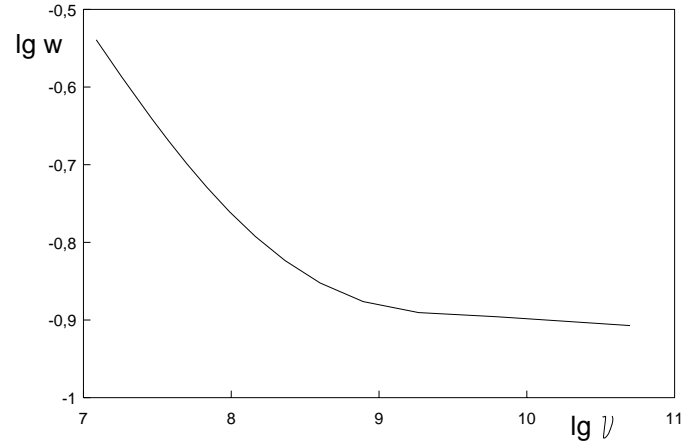


Fig. 5. Pulse half-width vs. frequency (plasma with outward density decrease); $\gamma = 30$, $\varepsilon = 3$, $\Omega_0 = 0.3$, $\kappa = 100$, $P = 1\text{s}$, $B_0 = 10^{12}\text{G}$

at low ones it increases. The pulse half-width versus frequency dependence calculated at $\Omega_0 = 0.3$, $\varepsilon = 3$ is shown in Fig. 5. The curve resembles those observed for many pulsars (Rankin 1983). Apparently, the frequency behaviour of the component separation in double profiles is to be similar to that plotted in Fig. 5. This agrees with observational data as well.

The rays propagating in the plasma with density decreasing towards the magnetic axis are found to suffer significant deviation towards the magnetic axis. For the rays emitted at small polar angles ($\vartheta_0 \lesssim 1/\gamma$) the deviation turns out to be so large that the right-hand side of Eq. (3.5) is negative. The latter implies that the rays emitted at the right-hand side of the tube form the left-hand side of the observed pulse profile and *vice versa*. Obviously, in this case the absolute value of the right-hand side of Eq. (3.5) is observed as the pulse width. Thus refraction amplifies the pulse width decrease with frequency until the rays intersect the magnetic axis and w becomes negative. The rays which intersected the axis form the opposite side of the pulse profile; the stronger they deviate the larger the observed pulse width. However, the rays emitted at still higher frequencies have time to deviate in the opposite direction due to the oppositely directed transverse density gradient beyond the magnetic axis, so that the observed pulse width decreases again. The calculated frequency dependence of pulse half-width is given in Fig. 6. One can see that the curve forms a trough; so it seems to resemble the observed ones exhibiting the so called "absorption feature". Thus refraction of rays in the plasma with outward density increase may account for the "absorption feature". Recall that in the above consideration the observed pulse width was supposed to be determined by the behaviour of rays emitted at the chosen magnetic field line. It is clear that taking into account the deviation of all the rays emitted inside the tube results in flattening the trough in Fig. 6.

4. Discussion

We investigated refraction of an ordinary superluminal radio wave propagating through an ultrarelativistic plasma embed-

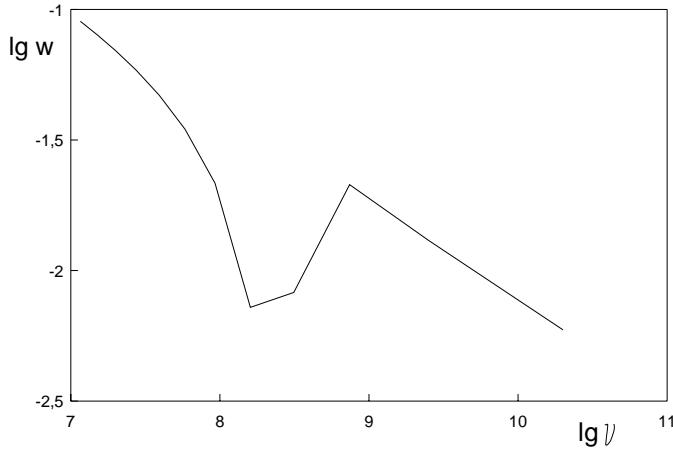


Fig. 6. Pulse half-width vs. frequency (plasma with outward density increase); $\gamma = 30$, $\varepsilon = 1$, $\Omega_0 = 0.3$, $\kappa = 30$, $P = 1$ s, $B_0 = 10^{12}$ G

ded in a superstrong dipole magnetic field. We assume that the frequency of the outgoing radio waves is of the order of (1.1) because induced scattering redistributes the waves in frequency towards this frequency. Our aim was to outline the main features of radio wave refraction and to analyse the observational consequences of the effect. Some simplifications are made in our research. Firstly, the plasma was supposed to be cold although it is not the case in pulsar magnetospheres. Secondly, we considered the rays which propagate in one of the planes containing the magnetic axis. These rays do form the observed pulse profile if the pulsar magnetic axis passes the line of sight. However, generally the line of sight scans the emission cone across a chord, the observed pulse width being formed by the rays deviating from the plane examined. Perhaps, considering refraction in the hot highly magnetized plasma involving three-dimensional geometry may lead to the results which are in better quantitative agreement with the observations. However, the qualitative picture of refraction is believed to be the same.

Refraction of a ray appears to occur mainly on account of plasma density gradient across the open field line tube. Outward density decrease causes ray deviation away from the magnetic axis while outward density increase makes the ray deviate towards the axis. Since the plasma flow widens along with the open field line tube transverse density gradient decreases with altitude, so that refraction becomes less efficient. Thus the latter is determined by the locus of the ray origin. Refraction is also found to depend upon the ratio of the frequency of the emitted wave to the local plasma frequency. The higher the frequency the slower the wave vector deviates and the earlier the wave decouples from the plasma and *vice versa*. It is shown that in the case of outward density increase, if refraction is efficient enough, (at low initial altitudes or at small dimensionless frequencies) the ray trajectory can cross the open field line tube for several times before the wave decouples from the plasma. The wave vector deviation then changes the sign causing the non-monotonic dependence of the final ray deviation on emission angle.

Refraction of rays in pulsar magnetospheres is found to be significant, so it influences the observed pulse widths. Since it depends essentially on the locus of the ray origin the pulse width versus frequency dependence is to differ from the $\nu^{-1/3}$ law. The pulse width calculated allowing for refraction in the plasma with outward density decrease turns out to be nearly constant at high frequencies and it increases at low ones. The pulse width versus frequency curve is compatible with those observed for many pulsars. Refraction of rays in the plasma with outward density increase leads to the following frequency behaviour of the pulse width. Decrease of pulse width at low frequencies is followed by the increase at higher ones; at still higher frequencies the pulse width decreases again. The calculated pulse width versus frequency curve seems to resemble the observed ones exhibiting the so called "absorption feature".

Note that relatively small plasma density corresponding to the multiplicity factor of $\sim 10^2$ (see Eq. (3.1)) turns out to be necessary for an agreement of the calculated curves with the observed ones. The κ values used to be obtained in the typical polar cap models are $\sim 10^3$ – 10^4 (Ruderman & Sutherland 1975; Arons & Scharlemann 1979; Arons 1983), however, all that considerations are rather rude and the values as low as $\sim 10^2$ cannot be excluded.

Acknowledgements. This work was partially supported by INTAS grant 94-3097.

References

- Arons J., 1983, ApJ 266, 215
- Arons J., Scharlemann E.T., 1979, ApJ 231, 854
- Barnard J.J., Arons J., 1986, ApJ 302, 138
- Bartel N., 1981, A&A 97, 384
- Blandford R.D., Scharlemann E.T., 1976, MNRAS 174, 59
- Bliokh K.Yu., Lyubarskii Yu.E., 1996, Pis'ma v Astron. Zh. 22, 539 [English translation: Astron. Lett. 22, 482 (1996)]
- Lyubarskii Yu.E., 1992a, A&A 261, 544
- Lyubarskii Yu.E., 1992b, A&A 265, L33
- Lyubarskii Yu.E., 1993, Pis'ma v Astron. Zh. 19, 34 [English translation: Astron. Lett. 19, 14 (1993)]
- Lyubarskii Yu.E., 1995, Astrophys. Space Phys. Rev. V.9, Pt.2, P.1
- Lyubarskii Yu.E., 1996, A&A 308, 809
- Mikhailovskii A.B., Onischenko O.G., Suramlishvili G.I., Sharapov S.E., 1982, Pis'ma v Astron. Zh. 8, 685
- Rankin J.M., 1983, ApJ 274, 359
- Ruderman M.A., Sutherland P.G., 1975, ApJ 196, 51
- Ursov V.V., Usov V.V., 1988, Ap&SS 140, 325
- Usov V.V., 1987, ApJ 320, 333